

SPG Mitteilungen Communications de la SSP

Auszug - Extrait

Progress in Physics (97)

Energy Thresholds in Plasma Sputtering Deposition

*Dirk Hegemann, Martin Amberg, Empa, Swiss Federal Laboratories for Materials Science and Technology,
Plasma & Coating Group, Lerchenfeldstrasse 5, CH-9014 St. Gallen (dirk.hegemann@empa.ch)*

This article has been downloaded from:
https://www.sps.ch/articles/progress_in_physics/

DOI: [10.5281/zenodo.10086365](https://doi.org/10.5281/zenodo.10086365)

Progress in Physics (97)

Energy Thresholds in Plasma Sputtering Deposition

Dirk Hegemann, Martin Amberg, Empa, Swiss Federal Laboratories for Materials Science and Technology, Plasma & Coating Group, Lerchenfeldstrasse 5, CH-9014 St. Gallen (dirk.hegemann@empa.ch)

Plasma sputtering deposition is a Physical Vapor Deposition (PVD) method based on a weakly ionized gas, the plasma, that ablates atoms from a solid target material to deposit those sputtered atoms on a substrate [1, 2]. In this way, the plasma has two functions, i) the generation of high-energy ions of several 100 eV accelerated to the target for sputtering, and ii) to support film growth by plasma-surface interaction with particles bearing lower energies around ~10 eV. For both processes, energy thresholds are present, which will be discussed in this article. Plasma sputtering deposition has wide spread industrial applications [3]. As one example, the metallization of polymer fibers is demonstrated to obtain electrically conductive textile sensors and wires [4-7].

Plasma sputtering at the target

The plasma used for sputtering is a gas discharge excited by electric or electromagnetic fields [8]. Electrons pick up energy from the field within collisions with the heavy gas particles, reaching electron energies of several eV (1 electron volt = $1.602 \cdot 10^{-19}$ J), while the gas particles largely remain at low temperatures resulting in highly non-equilibrium conditions. Due to the distribution of electron energies in the low temperature plasma, a sufficient amount of electrons gain energies to ionize the gas, and thus sustain the plasma by means of external power delivery. The mobile electrons tend to leave the plasma quickly, however, applying electromagnetic fields as used for the common magnetron sputtering process, electrons can be trapped for an extended time resulting in an increased electron density and ionization degree. Therefore, magnets are placed close to the target material to generate an intense plasma even at low pressure that is located just in front of the target [8]. Typically, pressures around 1 Pa are used to create sufficient ions but minimize collisions between the gas particles, which occur at a mean free path length of around 1 cm at such conditions. The high diffusion of electrons result in a net negative charging of surfaces exposed to the plasma, mainly at the target material yielding the high negative target voltage, V_t , while the plasma acquires a small positive potential, the plasma potential, V_{pl} . Between plasma and target, a potential drop is thus established ranging from tens to thousands of volts. Accordingly, positively charged ions created near the target are accelerated to ion energies, E_i , of tens to thousands of eV, assuming a collision-free sheath between plasma and target (as given at sufficient low pressure):

$$E_i = e(V_{pl} - V_t) \quad (1)$$

Related to the ion density, a flux of ions, Γ_i , is bombarding the target (with energies E_i) causing the sputtering yield, that is, the number of atoms released from the target material at the flux, Γ_{at} , per incident ion:

$$Y = \frac{\Gamma_{at}}{\Gamma_i} \quad (2)$$

To achieve a high momentum transfer, M_i , to the target material, sputtering is typically performed in heavy inert gases with ion masses, m_i :

$$M_i = \frac{\sqrt{2m_i E_i}}{Y} \quad (3)$$

The sputtering yield can be plotted vs. the ion energy as displayed in Figure 1a for different gases and target materials. At first, it can be noted that the onset of sputtering occurs with a threshold energy, $E_{th,s}$, typically around 50 eV [9]. Secondly, a range can be observed, where Y increases linearly with E_i , yielding a constant delivered energy, $E_{d,t}$, at the target material [10-13]:

$$E_{d,t} = \frac{E_i}{Y} \quad (4)$$

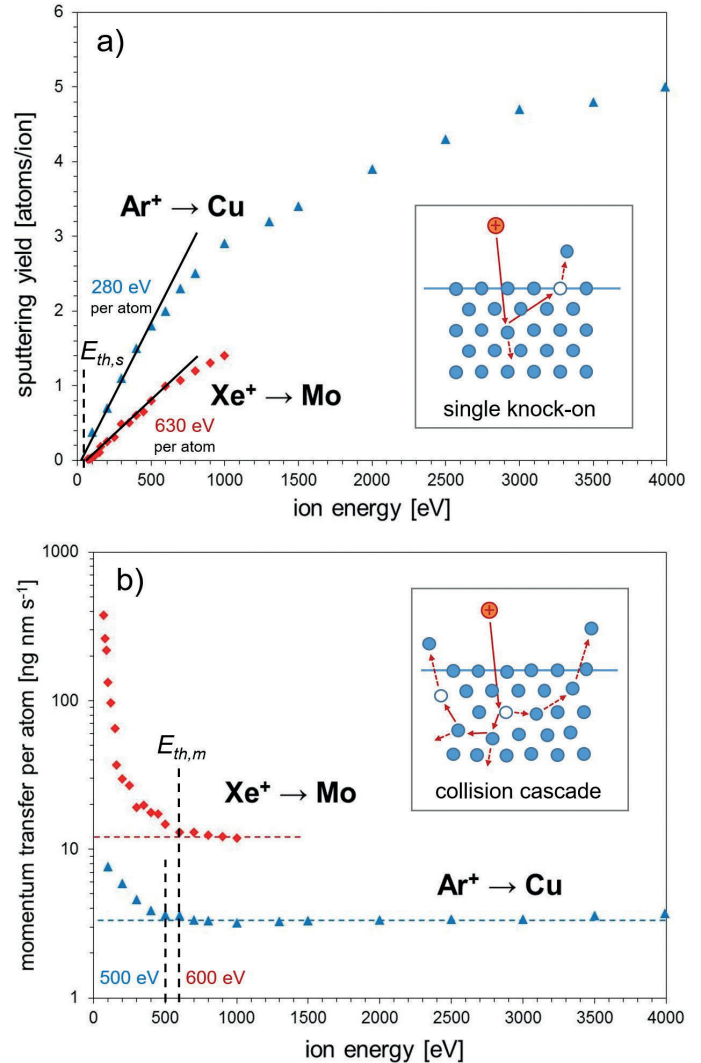


Figure 1: Sputtering in Ar and Xe plasmas with Cu and Mo target, respectively [11-13]. a) The sputtering yield increases linearly with ion energy above the threshold energy for sputtering, $E_{th,s}$, according to single knock-on processes. This regime is characterized by constant delivered energy per target atom. b) Above the threshold energy for predominant momentum transfer processes, $E_{th,m}$, sputtering is governed by collision cascades characterized by constant momentum transfer.

As seen in Figure 1b, only at enhanced ion energies, sputtering follows momentum transfer resulting in a constant M_i according to Equation (3). This regime, observed at a threshold energy, $E_{th,m}$, of 500 - 600 eV, is characterized by collision cascades transferring momentum between near-surface atoms [14]. For energetic reasons, however, plasma sputtering deposition is typically performed at ion energies below $E_{th,m}$, e.g. around 400 eV, to make use of the linear increase of Y with E_i . In this regime, sputtering is mainly caused by single knock-on events, transferring energy to a surface atom [10].

Plasma sputtering deposition

The sputtered atoms carry a surplus energy due to the sputtering process requiring to overcome the surface binding energy, which is, however, in the low eV range [2]. While those energies are sufficient to enhance surface diffusion of adsorbed sputtered atoms at the substrate material typically placed opposite to the target, film growth into a dense structure requires higher energies delivered to the growing film [8, 15]. At low energies below a threshold, $E_{th,b}$, of around 10 eV related to the surface binding energy, needle-like film morphologies containing voids are observed. Related structure zone models have been developed demonstrating different morphologies and crystallization induced by the delivered energy and the surface temperature with respect to the melting temperature of the deposited film as described in the literature [15].

The required energy can be delivered by the plasma, again through bombardment with energetic particles. While ions are accelerated towards the target gaining high energies of hundreds of eV, yielding the sputtering processes, they also interact with samples placed in the plasma zone. If such a sample is electrically insulated, its surface acquires a floating potential, V_f , that is more negative than the plasma potential, V_{pl} , due to the accumulation of mobile electrons from the plasma [16]. The resulting potential drop accelerating positive ions towards the sample is proportional to electron temperature, T_e (in [eV]):

$$V_{pl} - V_f = \frac{T_e}{2e} \cdot \ln\left(0.433 \frac{m_i}{m_e}\right) \quad (5)$$

The \ln term given by the ratio of ion to electron mass, m_i and m_e , respectively, is not much varying for different ions, lying around 10. As an example, in an Ar plasma at a pressure of 2 Pa, the potential drop (using a Retarded Field Energy Analyzer) was measured to be about 20 V, yielding $T_e \approx 4$ eV for the used plasma conditions, largely independent of delivered power. Ar ions are thus accelerated to $E_i \approx 20$ eV, noting that the thin sheath of ~ 1 mm around the floating sample is collision-free. With the known flux of ions, Γ_i , incident on the sample, the delivered energy, E_d , can be estimated by

$$E_d = E_i \frac{\Gamma_i}{R} \quad (6)$$

with the film growth rate, R (in [atoms $\text{cm}^{-2} \cdot \text{s}^{-1}$]), determined by the flux of sput-

tered atoms that adsorb at the sample. Γ_i can be assessed by measuring the electron density, n_e , at different distances in front of the target (using Microwave Interferometry which integrates over about 1 - 2 cm width). Due to quasi-neutrality, the ion density is given by $n_i = n_e$. As depicted in Figure 2, n_i is highest in front of the target, separated by the plasma sheath (of about 1 cm width at a pressure of 2 Pa), and decreases with increasing distance. By placing samples at varying distance, the ion bombardment, also inducing heat load, can thus be adjusted. Note that the target needs to be cooled, whereas temperature-sensitive samples at floating potential can only be placed at a sufficient distance from the target.

Taking the initial velocity of ions, the Bohm velocity, v_B , required to enter the sheath, and diffusion by collisions in the plasma into account [16], it follows that

$$\Gamma_i \approx 0.5 \cdot v_B \cdot n_i \quad (7)$$

By measuring the deposition rate and using Eq. (5), (6), and (7), the deposited energy can eventually be calculated. Figure 2 shows an example of coating polymer fibers that are guided in front of a silver target to be metallized by magnetron sputtering [17]. Increasing the applied power enhances the sputtering yield by increasing the potential drop in front of the target according to Eq. (1) and (4) (within the single knock-on regime). Moreover, the electron density (and thus ion density) scales with applied power, thus enhancing the ion flux resulting in strongly increased deposition rates (Figure 2c). Since the ion density is reduced with distance to the target, the deposited energy (Eq. (6)) can be adjusted by placing the samples at different positions in the plasma chamber. Due to the heat load by the plasma, polymer samples need to have a sufficient distance. For example, sample placement 9 cm from the target limits the heat load to about 50 - 60°C. On the contrary, high-quality film growth assuring excellent adhesion requires a threshold energy overcoming the surface binding energy of about 10 eV [18]. As can be seen from Figure 2c, the two examined conditions at high and low power supply enable $E_d > E_{th,b}$, where the higher power allows the higher process velocity. Note that closer placement of the samples could also result in conditions meeting (again) the threshold for sputtering at around 50 eV. The deposited energy should thus be well controlled. The

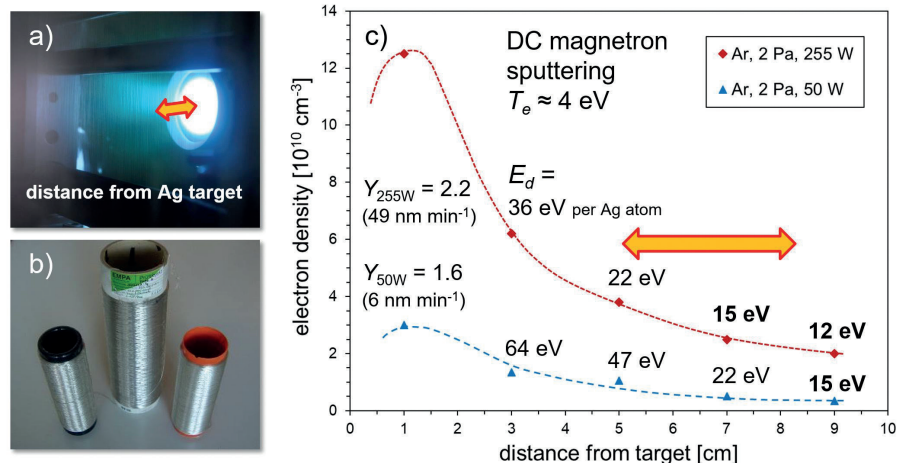


Figure 2: Plasma sputtering deposition of silver films on fibers. a) The fibers are moved in front of the target at a variable distance. b) Ag-coated (metallized) fibers as produced by sputtering. c) Measurement of electron densities at different distances from the target, which agrees with ion density, to calculate the deposited energy, E_d , during film growth.

electrical conductivity of the Ag-coated fibers can then be adjusted by the thickness of the deposited metal film, typically 100 - 500 nm [4]. For the optimized conditions with $R \approx 49 \text{ nm min}^{-1}$, a residence time of 2 - 10 min of the fiber in the plasma zone is thus required. At industrial scale, about 2 km of fiber is introduced in the plasma by winding from reel to reel yielding a typical process velocity of 200 - 1000 m min^{-1} . A yarn material with 200 dtex (weighing 200 g per 10000 m fiber length) thus requires a processing time of about 1-4 hrs to produce 1 kg of material, which is economically feasible.

The metallized fibers are used for various applications including products used in healthcare such as antimicrobial textiles and textile electrodes for ECG measurements [5, 7]. Recent developments deal with the manufacturing of a rope that comprises coated and uncoated fibers of the same type, e.g. high-strength Twaron® fibers, allowing an inherent sensor function (Figure 3). Using the electrical resistivity of the rope as indicator for the abrasion of the rope in load-bearing applications, the end-of-life can be predicted. X-ray micro tomography (μCT) analysis [19] demonstrates that the metal coating survives the abrasion process, while the polymer fibers show wear such as broken filaments that contribute to an increase in resistivity.

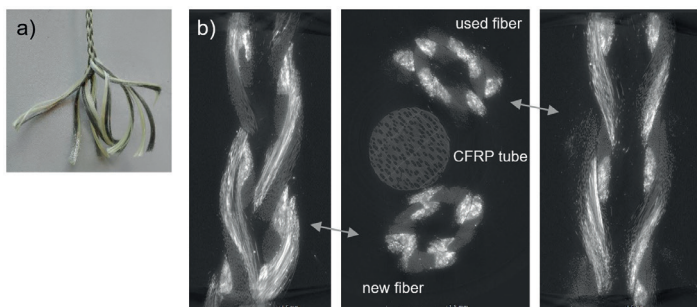


Figure 3: a) Rope made of 8x2 Twaron® fibers by twisting two parallel fibers, one Ag-coated and one uncoated. b) μCT imaging of the rope as prepared (new fiber) and after extensive abrasion testing (used fiber) in cross section (middle, separated by a carbon fiber-reinforced polymer tube) and along the rope (sides).

Furthermore, metallized fibers can be plied together to enhance electrical conductivity reaching values below $100 \Omega \text{ m}^{-1}$. Using a high-strength polymer fiber such as Vectran™, a flexible and light-weight textile wire can be manufactured that is protecting its conductive, metallized core fibers by an outer shell of uncoated fibers of the same type using textile braiding (Figure 4). These wires can be used to transfer data but also as reference wire, stretched over more than hundred meter as used for the alignment of linear accelerators [20].

Conclusions

Plasma sputtering deposition is a mature physical vapor deposition technology that can also be used to metallize polymers by controlling sputtering conditions at the target material (selecting the type of coating) and at the polymer substrate in order to reduce heat load. Different energy thresholds can be identified yielding both an optimum window for sputtering at the target and deposition on the polymer. Here, silver coatings on continu-

ous polymer fibers were discussed that can be deposited in a reel-to-reel process resulting in electrically conductive fibers. From these fibers, ropes and textile wires can be manufactured allowing, for example, the transfer of data and sensor applications.

Acknowledgements

The Innosuisse-funded projects 25101.1 PFIW-IW and 28736.1 IP-ENG are gratefully acknowledged.

References

[1] S. M. Rossnagel, *J. Vac. Sci. Technol. A* **21**, S74–S87 (2003)
 [2] W. D. Westwood, *Sputter Deposition*, AVS, USA (2003)
 [3] A. Baptista, F. J. G. Silva, J. Porteiro, J. L. Miguez, G. Pinto, *Proc. Manufacturing* **17**, 746–757 (2018)
 [4] M. Amberg, K. Grieder, P. Barbadoro, M. Heuberger, D. Hegemann, *Plasma Process. Polym.* **5**, 874–880 (2008)
 [5] D. Hegemann, M. Amberg, A. Ritter, M. Heuberger, *Mater. Technol.* **24**, 41–45 (2009)
 [6] M. Amberg, C. Kasdallah, A. Ritter, D. Hegemann, *J. Adhesion Sci. Technol.* **24**, 123–134 (2010)
 [7] M. Amberg, P. Rupper, R. Storchenegger, M. Weder, D. Hegemann, *Nanomed. Nanotechnol. Biol. Med.* **11**, 845–853 (2015)
 [8] A. Anders, *J. Appl. Phys.* **121**, 171101 (2017)
 [9] I. I. Amirov, M. O. Izyumov, V. V. Naumov, E. S. Goralchev, *J. Phys. D: Appl. Phys.* **54**, 065204 (2021)
 [10] P. Sigmund, in: *Sputtering by Particle Bombardment*, Vol. I, ed. R. Behrisch, Springer-Verlag, Berlin, Germany, pp 9–71 (1981)
 [11] M. Koedam, *Physica* **24**, 692–694 (1958)
 [12] H. K. Pulker, *Coatings on Glass*, Elsevier, Amsterdam, The Netherlands, p. 216 (1984)
 [13] R. D. Kolasinski, J. E. Polk, D. Goebel, L. K. Johnson, *J. Vac. Sci. Technol. A* **25**, 236–245 (2007)
 [14] M. P. Seah, *Nucl. Instr. Meth. Phys. Res. B* **229**, 348–358 (2005)
 [15] A. Anders, *Thin Solid Films* **518**, 4087 (2010)
 [16] M. A. Lieberman, A. J. Lichtenberg, *Principles of Plasma Discharges and Materials Processing*, John Wiley & Sons, New York, USA (1994)
 [17] D. Hegemann, B. Hanselmann, N. Blanchard, M. Amberg, *Contr. Plasma Phys.* **54**, 162–169 (2014)
 [18] D. Hegemann, *Plasma Polymer Deposition and Coatings on Polymers*. In: *Comprehensive Materials Processing*, Vol. 4, Ed. D. Cameron, Elsevier Ltd. pp 201–228 (2014)
 [19] S. Iswar, M. Griffa, R. Kaufmann, M. Beltran, L. Huber, S. Brunner, M. Lattuada, M. M. Koebel, W. J. Malfait, *Micropor. Mesopor. Mater.* **278**, 289–296 (2019)
 [20] T. Touzé, H. Mainaud Durand, *Proc. Particle Accelerator Conference, PAC09*, Vancouver, Canada (2010)

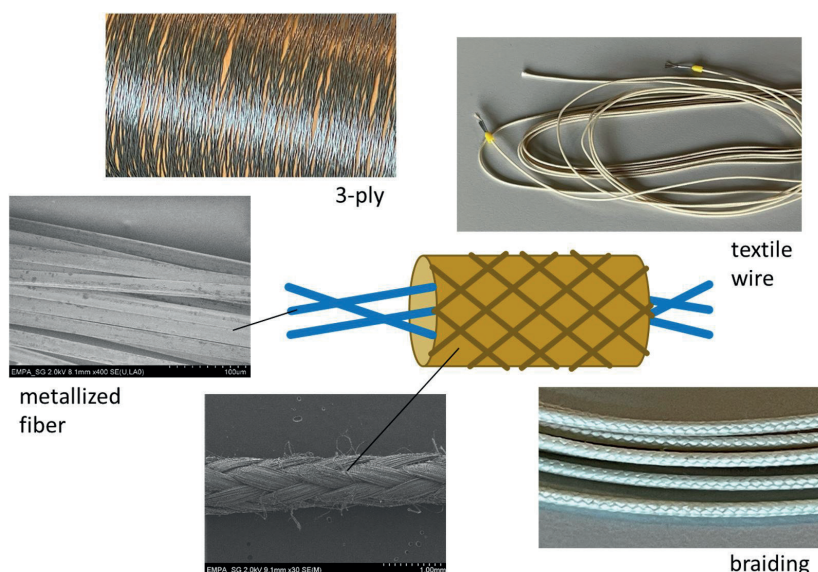


Figure 4: High-strength textile wire made of three Ag-coated Vectran™ fibers, plied together (3-ply), as electrically conductive core, which is protected by six (uncoated) Vectran™ fibers using textile braiding.